In vitro and *in vivo* activity of R547: a potent and selective cyclin-dependent kinase inhibitor currently in phase I clinical trials

Wanda DePinto,[1] Xin-Jie Chu,[2] Xuefeng Yin,[1] Melissa Smith,[1] Kathryn Packman,[1] Petra Goelzer,[3] Allen Lovey,[2] Yingsi Chen,[4] Hong Qian,[4] Rachid Hamid,[4] Qing Xiang,[4] Christian Tovar,[1] Roger Blain,[3] Tom Nevins,[1] Brian Higgins,[1] Leopoldo Luistro,[1] Kenneth Kolinsky,[1] Bernardo Felix,[1] Sazzad Hussain,[3] and David Heimbrook[1]

[1]Discovery Oncology, [2]Discovery Chemistry, [3]Non-Clinical Drug Safety, and [4]Discovery Technology, Hoffmann-La Roche, Inc., Nutley, New Jersey

Abstract

The cyclin-dependent protein kinases are key regulators of cell cycle progression. Aberrant expression or altered activity of distinct cyclin-dependent kinase (CDK) complexes results in escape of cells from cell cycle control, leading to unrestricted cell proliferation. CDK inhibitors have the potential to induce cell cycle arrest and apoptosis in cancer cells, and identifying small-molecule CDK inhibitors has been a major focus in cancer research. Several CDK inhibitors are entering the clinic, the most recent being selective CDK2 and CDK4 inhibitors. We have identified a diaminopyrimidine compound, R547, which is a potent and selective ATP-competitive CDK inhibitor. In cell-free assays, R547 effectively inhibited CDK1/cyclin B, CDK2/cyclin E, and CDK4/cyclin D1 (K_i = 1–3 nmol/L) and was inactive (K_i > 5,000 nmol/L) against a panel of >120 unrelated kinases. *In vitro*, R547 effectively inhibited the proliferation of tumor cell lines independent of multidrug resistant status, histologic type, retinoblastoma protein, or p53 status, with IC_{50}s ≤ 0.60 μmol/L. The growth-inhibitory activity is characterized by a cell cycle block at G_1 and G_2 phases and induction of apoptosis. R547 reduced phosphorylation of the cellular retinoblastoma protein at specific CDK phosphorylation sites at the same concentrations that induced cell cycle arrest, suggesting a potential pharmacodynamic marker for clinical use. *In vivo*, R547 showed antitumor activity in all of the models tested to date, including six human tumor xenografts and an orthotopic syngeneic rat model. R547 was efficacious with daily oral dosing as well as with once weekly i.v. dosing in established human tumor models and at the targeted efficacious exposures inhibited phosphorylation of the retinoblastoma protein in the tumors. The selective kinase inhibition profile and the preclinical antitumor activity of R547 suggest that it may be promising for development for use in the treatment of solid tumors. R547 is currently being evaluated in phase I clinical trials. [Mol Cancer Ther 2006;5(11):2644–58]

Introduction

Cyclin-dependent kinases (CDK) are serine/threonine kinases that regulate cell cycle progression in a coordinated fashion (1). These enzymes are activated by formation of complexes with proteins known as cyclins. Whereas CDK levels remain constant during the cell cycle, cyclin levels fluctuate, and the phases of the cell cycle are controlled by activation of different CDK-cyclin complexes. In early to mid G_1, activation of CDK4/cyclin D1 and CDK6/cyclin D3 induces phosphorylation of the retinoblastoma protein. Phosphorylation of retinoblastoma releases the transcription factor E2F, which enters the nucleus and activates transcription of cyclin E and cyclin A. CDK2/cyclin E promotes progression through S phase, along with additional phosphorylation of retinoblastoma and further E2F release. CDK2/cyclin A also phosphorylates several substrates, leading to DNA replication. CDK1/cyclin B mediates the transition into M phase and completes mitosis (2, 3). These CDK-cyclin complexes are further regulated by the endogenous CDK inhibitors *p16, p15, p19, p21, p27*, and *p57*, and mutations and deletions of these genes are found in many human cancers (4).

Dysregulation of cell cycle progression is a universal characteristic of cancer cell proliferation, and the majority of human cancers have abnormalities in some component of the pathway. Therefore, there is interest in developing small-molecule pharmacologic CDK inhibitors to block cell cycle progression to inhibit tumor growth (5–7), and CDK1, CDK2, and CDK4 have been targeted for small-molecule inhibitor development (8–11). CDK4 inhibitors have been considered as prime targets for cancer chemotherapy for many years (12, 13), although more recently CDK4 has been linked to modulation of cell growth rate in *Drosophila*, and it has been suggested that CDK4 is dispensable for cell cycle progression (14). The importance of CDK4, however, in regulation of the tumor cell cycle is evident in knock-in mice where the normal *CDK4* gene is

Received 6/20/06; revised 8/11/06; accepted 9/12/06.

The costs of publication of this article were defrayed in part by the payment of page charges. This article must therefore be hereby marked advertisement in accordance with 18 U.S.C. Section 1734 solely to indicate this fact.

Requests for reprints: Wanda DePinto, Discovery Oncology, Hoffmann-La Roche, Inc., 340 Kingsland Street, Nutley, NJ 07110. Phone: 973-235-2866; Fax: 973-235-6185. E-mail: wanda.depinto@roche.com

doi:10.1158/1535-7163.MCT-06-0355

replaced by a CDK4 mutant insensitive to endogenous CDK inhibitors. The animals develop a wide spectrum of spontaneous tumors and are highly susceptible to specific carcinogenic treatments (15). The need for CDK2 and cyclin E complexes for cell proliferation and validity of CDK2 as a drug target has also being questioned. Mammalian cells can proliferate in the absence of CDK2/cyclin E activity, and it has been speculated that other CDKs may compensate for CDK2 (16, 17). Still, other reports raise the possibility that CDK2 selective inhibitors may preferentially induce apoptosis in tumor cells (18, 19). CDK1 inhibition is reportedly not well tolerated by cells and also leads to apoptotic cell death, suggesting that selective CDK1 inhibition may be an attractive anticancer therapy (20). Recently, CDK1/cyclin E complexes have been shown to regulate the G_1-S phase transition in the absence of CDK2 and compensate for compromised CDK2 function (21, 22).

Some of the CDK inhibitors recently entering clinical trials also inhibit CDK5, CDK7, and CDK9, which have functions not directly involving the cell cycle. CDK5 is important in regulating insulin secretion, synaptic vesicle recycling, neuronal survival, and τ phosphorylation and aggregation (23) and also reportedly regulates cell adhesion and migration in epithelial cells (24). CDK7 and CDK9 regulate RNA transcription via phosphorylation of RNA polymerase II, and it is suggested that inhibiting either CDK7 or CDK9 may contribute to antitumor activity. Induction of cell death in tumor cells by inhibition of RNA polymerase II–dependent transcription and down-regulation of the antiapoptotic protein Mcl-1 has been reported for several agents (25, 26).

Although significant progress has been made in targeting the CDKs, questions about the importance of CDK selectivity for effective tumor growth inhibition (TGI) remain. Absolute selectivity may not be the best approach to treat complex disorders where multiple pathways are deregulated, and combinations of effects might provide for better therapeutic agents. A broad-spectrum CDK inhibitor that selectively inhibits several CDKs may have enhanced antitumor activity.

In this report, we describe the identification of a diaminopyrimidine compound, R547, a potent and highly selective ATP-competitive inhibitor of the CDKs. *In vitro*, R547 inhibited the proliferation of tumor cell lines and was active in all 19 cell lines tested irrespective of tissue of origin, multidrug resistance (MDR), p53, or retinoblastoma status. *In vivo*, R547 caused significant TGI in all of the models tested when dosed orally and i.v. at or below the maximum tolerated dose. At the efficacious exposures in tumor xenograft models, R547 inhibited phosphorylation of retinoblastoma protein in tumors, providing a pharmacodynamic biomarker for clinical use. The selective kinase inhibition profile and the preclinical antitumor activity of R547 reported here suggest that this is a promising molecule for evaluation in the treatment of solid tumors. Phase I clinical trials of R547 have been initiated.

Materials and Methods

Reagents

R547, [4-amino-2-(1-methanesulfonylpiperidin-4-ylamino) pyrimidin-5-yl]-(2,3-difluoro-6-methoxyphenyl) methanone, was synthesized by Discovery Chemistry, Hoffmann-La Roche, Inc. (Nutley, NJ; Fig. 1A). The chemistry and synthesis of R547 will be described separately.[5] Paclitaxel (Taxol) and doxorubicin were purchased from Sigma (St. Louis, MO). To prepare stock solutions, compounds were dissolved at 10 or 30 mmol/L in 100% DMSO (Sigma) and stored at −20°C in amber glass vials.

Expression and Purification of CDK, Cyclin, and Retinoblastoma Proteins

Recombinant human CDK1, CDK2, and CDK4-cyclin complexes were expressed in insect cells and purified as described previously (27). A 6× histidine-tagged truncated form of retinoblastoma protein (amino acids 386–928) was used as the substrate, the expression plasmid, kindly provided by Dr. Veronica Sullivan (Department of Molecular Virology, Roche Research Centre, Welwyn Garden City, United Kingdom). The expression and purification of the 62-kDa retinoblastoma protein was carried out as described previously (27).

Kinase Assays

Enzyme reactions were initiated by adding recombinant histidine-tagged enzyme and retinoblastoma substrate to 384-well plates containing diluted test compounds. Final reaction conditions were such that the ATP concentration was 3× the respective enzyme K_m for ATP in the presence of 25 mmol/L HEPES (pH 7.0), 6.25 mmol/L $MgCl_2$, 1.5 mmol/L DTT, 0.002% Tween 20, and 0.2 mg/mL bovine serum albumin (BSA). After a 25-minute incubation at 37°C, reactions were terminated by addition of anti-phosphorylated retinoblastoma (Ser^{780}) antibody (Cell Signaling Technology, Beverly, MA). The phosphorylated retinoblastoma was analyzed by adding lance europium anti-rabbit IgG and anti-His-allophycocyanin, resulting in fluorescence resonance energy transfer between europium anti-rabbit and allophycocyanin, and quantified by fluorescence intensity ratio 665 nm/615 nm (excited at 340 nm). IC_{50}s were calculated from net readings at 665 nm, normalized for europium readings at 615 nm. The kinase insert domain-containing receptor, fibroblast growth factor receptor, platelet-derived growth factor receptor, and epidermal growth factor receptor kinase assays are also homogeneous time-resolved fluorescence assays. Protein kinase A, protein kinase B, protein kinase Cα, protein kinase Cβ, FYN, extracellular signal-regulated kinase 2, p38, mitogen-activated protein kinase 2, serum/glucocorticoid-regulated kinase, and EPHB3 assays were conducted

[5] X-J. Chu, W. De Pinto, D. Bartkovitz, et al. Discovery of [4-amino-2-(1-methanesulfonylpiperidin-4-ylamino) pyrimidin-5-yl]-(2, 3-difluoro-6-methoxyphenyl) methanone (R547), a potent and selective cyclin dependent kinase inhibitor with significant *in vivo* antitumor activity. J Med Chem. In press 2006.

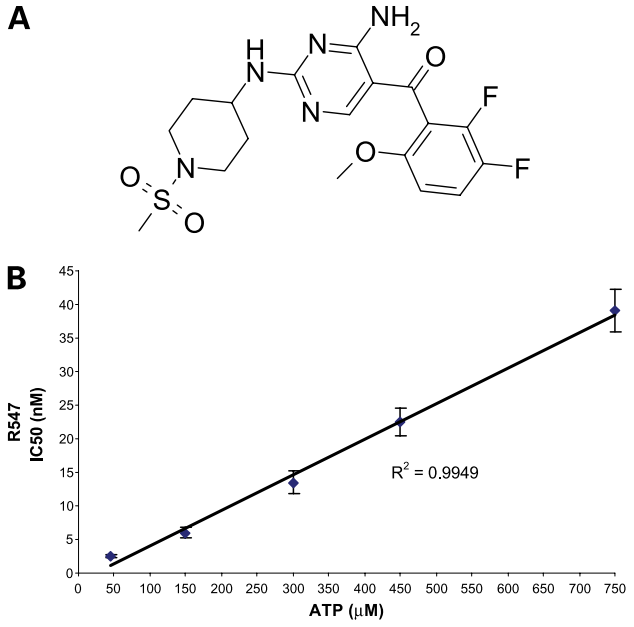

Figure 1. **A,** chemical structure of R547, [4-amino-2-(1-methanesulfonylpiperidin-4-ylamino) pyrimidin-5-yl]-(2,3-difluoro-6-methoxyphenyl) methanone. **B,** IC_{50} for inhibition of recombinant human CDK4/cyclin D1 by R547 was calculated at increasing concentrations of ATP and produced a linear relationship relative to total ATP concentration. At each concentration, $n = 4$; *bars,* SD.

using an assay based on IMAP Technology (Molecular Devices Corp., Sunnyvale, CA) that enables quantitation of kinase activity via preferential binding of phosphorylated fluorescent peptide substrates to immobilized metal beads. These reactions were carried out at ATP concentrations of 3× the K_m for the respective enzyme. SRC, focal adhesion kinase, AURORA, glycogen synthase kinase (GSK) 3β, and insulin-like growth factor receptor kinase assays are fluorescence resonance energy transfer assays run at the K_m for ATP. R547 was also evaluated for activity against 123 kinases at a single 10 μmol/L concentration in the Upstate kinase selectivity screen (Kinase Profiler, Kinase Profiler-FP, and PI Profiler, Upstate Biotechnology, Lake Placid, NY), and the IC_{50}s determined in the Upstate IC_{50} Profiler Express for kinases identified as hits in the initial screen.

Cell Culture

Cell lines were maintained in the recommended medium and supplemented with 10% heat-inactivated fetal bovine serum (Life Technologies, Gaithersburg, MD) and 2 mmol/L L-glutamine (Life Technologies). KB-A-1 cells were continuously maintained in 1 μg/mL doxorubicin. All media were from Life Technologies. The KB-3-1 and KB-A-1 cell lines (28) were from Dr. Michael M. Gottesman (National Cancer Institute, Bethesda, MD). SW480 cells were provided by Dr. Bert Vogelstein (Johns Hopkins University, Baltimore, MD; ref. 29), and MDA-MB-435 cells were provided by Dr. Patricia Steeg (National Cancer Institute) upon permission of Dr. Janet Price (University of Texas M.D. Anderson Cancer Center, Houston, TX; ref. 30). MTLn3 cells were from Dr. Anthony Neri (Department of Oncology, Hoffmann-La Roche; ref. 31). The H460a cell line was a generous gift from Dr. Jack Roth (University of Texas M.D. Anderson Cancer Center; ref. 32). The LOX IMVI cells were provided by the Biological Testing Branch, Developmental Therapeutics Program, Division of Cancer Treatment and Diagnosis, National Cancer Institute-Frederick Cancer Research and Development Center (Frederick, MD). The Mat-Lylu cells were from the European Collection of Animal Cell Cultures (Salisbury, Wiltshire, United Kingdom). The JEKO-1 and REC-1 cells were from the Deutsche Sammlung von Mikroorganismen und Zellkulturen GmbH (Braunschweig, Germany). All other cell lines were obtained from the American Type Culture Collection (Rockville, MD).

Tetrazolium Dye Proliferation [3-(4,5-Dimethylthiazol-2-yl)-2,5-Diphenyltetrazolium Bromide] Assay

Proliferation was evaluated by the tetrazolium dye assay according to the procedure of Denizot and Lang (33), and assays were done as described previously (34).

Analysis of Cell Cycle Distribution

The effect of the compound on cell cycle progression was determined using dual-variable flow cytometry. Cells were labeled with propidium iodide and bromodeoxyuridine (BrdUrd) to measure both the DNA and BrdUrd contents of the cells. A modification of the method as described by Bussink et al. (35) was followed for determination of percentage cells in S phase. Cells were plated in 10-cm dishes at 5×10^4/mL in 10 mL of growth medium and incubated at 37°C with 5% CO_2. After 24 hours, 30 μL of a stock solution of the test compound in 100% DMSO were added to individual dishes to obtain a final concentration equivalent to the IC_{50}, IC_{90}, and $3 \times IC_{90}$ of the compound as determined in antiproliferative assays. To the control dish, 30 μL of 100% DMSO were added (final concentration of DMSO in all plates is 0.3%). Cells were pulsed with 20 μmol/L BrdUrd for 1 hour before harvesting, and supernatant and cells were collected at the indicated time points. Cells were resuspended in 0.5 mL ice-cold PBS and fixed by slow addition of 5 mL ice-cold 70% ethanol while vortexing. Cells were washed twice with PBS and resuspended in 1 mL of a 2 N HCl/0.5% Triton X-100 solution for 30 minutes at room temperature. After centrifugation, 1 mL of 0.1 mol/L $Na_2B_4O_7$ was added to the pellet and cell nuclei were washed with PBS, resuspended in 100 μL of 0.5% Tween 20/1% BSA/PBS containing 20 μL of anti-BrdUrd FITC (Becton Dickinson, San Jose, CA), and incubated in the dark for 30 minutes.

Samples were washed with the Tween 20/BSA/PBS buffer, resuspended in 500 μL PBS containing 50 μg of propidium iodide (Sigma), and analyzed by flow cytometry.

Mitotic Protein Monoclonal 2 Staining

For staining of cells with both propidium iodide and mitotic protein monoclonal 2 (MPM2) antibody, the procedure of Andreassen and Margolis was followed (36). Cells were prepared and treated with R547 as described for cell cycle analysis. After removal of the ethanol by

centrifugation and aspiration, cells were resuspended in 0.5 mL PBS containing 3% BSA with 0.05% Tween 20. MPM2 antibody (200 μg; Upstate Biotechnology) was added and incubated with the cells at 37°C for 1 hour. Cells were washed twice with PBS and resuspended in 0.5 mL PBS containing 3% BSA with 0.05% Tween 20. FITC-conjugated $F(ab')_2$ fragment goat anti-mouse IgG (5 μg; 1:100 dilution; Jackson ImmunoResearch, West Grove, PA) was added, and cells were incubated for 30 minutes at 37°C. Cells were washed twice with PBS, treated with RNase A and propidium iodide, and analyzed by flow cytometry.

DNA Fragmentation

The proportion of cells with DNA fragmentation was determined using the APO-BRDU assay kit (Phoenix Flow Systems, Inc., San Diego, CA), which labels DNA breaks and total cellular DNA. Cells were exposed to a concentration of compound equivalent to the IC_{50}, IC_{90}, and $3 \times IC_{90}$, and control cells were treated with DMSO. After 24 to 72 hours, cells were fixed in 1% (w/v) paraformaldehyde, washed in PBS, and stored in 70% (v/v) ethanol at −20°C. To detect percentage apoptotic cells, the samples were processed according to the manufacturer's protocol and analyzed by flow cytometry.

Protein Extraction and Western Blot Analysis

Cells were washed thrice with cold PBS on ice, scraped from the flasks, and pelleted by centrifugation, and lysis buffer was added [1:1 PBS/2× Tris-glycine SDS sample buffer (Invitrogen, Carlsbad, CA) containing 5% β-mercaptoethanol]. The volume of lysis buffer was 5 μL per 1×10^6 cells. Samples were sonicated for 30 seconds on ice and clarified by centrifugation at 16,000 × *g* for 10 minutes at 4°C, and protein concentrations were determined using Non-Interfering Protein Assay kit (Geno Technology, Inc., Maplewood, MO). Tumor lysates were prepared by homogenizing the tumor in lysis buffer and clarifying by centrifugation as described above. Proteins were denatured by boiling for 5 minutes. Proteins were resolved (20–40 μg of cell lysate per lane) by SDS-PAGE using a 4% to 12% Tris-glycine gel (Invitrogen) and transferred to a polyvinylidene difluoride membrane (Invitrogen). Membranes were blocked for 1 hour at room temperature in blocking buffer (5% milk in PBS/0.1% Tween 20) followed by incubation with the primary antibody at 4°C overnight. Membranes were washed and incubated with the secondary antibody for 30 minutes at room temperature, and immunodetection was carried out using enhanced chemiluminescence (ECL Plus Reagent, Amersham Pharmacia Biotech, Piscataway, NJ). For Western blotting, total retinoblastoma was detected using antibody from PharMingen (BD Biosciences, San Diego, CA) at a dilution of 1:2,000. The phosphorylation status of retinoblastoma in the tumor and cell lysates was detected using a polyclonal antibody prepared against a peptide corresponding to a sequence surrounding phosphorylated Ser^{795}, Ser^{780}, Ser^{807}/Ser^{811} (Cell Signaling Technology), and Thr^{821} (BioSource International, Camarillo, CA) in human retinoblastoma. Actin was used for standardization of protein loading.

Xenograft Studies

Female immunodeficient nude mice (10 per group), obtained from Charles River Laboratories (Wilmington, DE), were used when approximately 13 to 14 weeks old and approximately 23 to 25 g. Autoclaved water and irradiated food were provided *ad libitum*, and animals were maintained on a 12-hour light and 12-hour dark cycle. Cages, bedding, and water bottles were autoclaved before use and changed weekly. Female Fischer rats (10 per group), also obtained from Charles River Laboratories, were used when 13 to 14 weeks old and ~150 g. The health of all animals was determined by daily gross observation of experimental animals, and analyses of blood samples of sentinel animals housed on shared shelf racks. All animals were allowed to acclimate and recover from any shipping-related stress for a minimum of 72 hours before experimental use. All animal experiments were done in accordance with protocols approved by the Roche Animal Care and Use Committee. The HCT116 cells (3×10^6 per mouse), H460a cells (1×10^7 per mouse), MDA-MB-435 cells (1×10^7 per mouse), DU145 cells (5×10^6 per mouse), LOX cells (2×10^6 per mouse), and A549 cells (7.5×10^6 per mouse) were implanted s.c. in the right flank. The cells were implanted in 0.2 mL PBS, except for the DU145 and MDA-MB-435 cells that were resuspended in 1:1 Matrigel/PBS. MTLn3 cells were implanted (1×10^6 per rat in PBS) s.c. in the right inguinal mammary fat pad. Animals were randomized according to tumor volume so that all groups have similar mean tumor volumes of approximately 100 to 150 mm^3. Doses selected were based on previously determined maximum tolerated doses. Oral R547 was formulated as a suspension in Klucel LF/Tween 80, and i.v. R547 was formulated as a solution in hydroxylpropyl β-cyclodextrin, sodium hydroxide, and water for i.v. injection. Tumor measurements and animal weights were taken on average thrice weekly, and all animals are individually followed throughout the experiment. Weight loss was calculated as percentage change in mean group body weight using the following formula: $[(W - W_0) / W_0] \times 100$, where '$W$' represents mean body weight of the treated group at a particular day and 'W_0' represents mean body weight of the same treated group at initiation of treatment. Efficacy data are graphically represented as the mean tumor volume + SE. Tumor volumes of treated groups are presented as percentages of tumor volumes of the control groups (%T/C) using the following formula: $100 \times [(T - T_0) / (C - C_0)]$, where T represented mean tumor volume of a treated group on a specific day during the experiment, T_0 represented mean tumor volume of the same treated group on the first day of treatment, C represented mean tumor volume of a control group on the specific day during the experiment, and C_0 represented mean tumor volume of the same treated group on the first day of treatment. Tumor volumes (in mm^3) were calculated using the following ellipsoid formula: $[D \times (d^2)] / 2$, where 'D' represents the large diameter of the tumor and 'd' represents the small diameter. Statistical analysis is done using the rank sum

Table 1. Kinase activity of R547

A. Inhibitory activity of R547 against a panel of in-house protein kinases

Kinase	K_i* (nmol/L) ± SD
CDK4/cyclin D1	1 ± 0.1
CDK2/cyclin E	3 ± 0.8
CDK1/cyclin B	2 ± 0.8
PKA	>5,000
PKB	>5,000
PKCα	>5,000
PKCβ	>5,000
FYN	>5,000
EPHB3	>5,000
SGK	>5,000
p38	>50,000
GSK3β	8,000
KDR	>5,000
FGFR	>5,000
EGFR	>5,000
PDGF	>5,000
MAPK2	>50,000
IGFR	>5,000
SRC	>5,000
FAK	>5,000
AURORA	>5,000

B. Inhibitory activity of R547 in the Upstate kinase selectivity screen

Kinase	IC_{50} (nmol/L)	Kinase	IC_{50} (nmol/L)	Kinase	IC_{50} (nmol/L)
CDK2/cyclin A	0.1	FGFR3	>10,000	PKA	>10,000
CDK2/cyclin E	0.4	FGFR4	>10,000	PKBβ	>10,000
CDK1/cyclin B	0.2	Flt1	>10,000	PKBγ	>10,000
CDK3/cyclin E	0.8	Flt3	>10,000	PKCα	>10,000
CDK5/p35	0.1	Fms	>10,000	PKCβI	>10,000
CDK6/cyclin D3	4.0	Fyn	>10,000	PKCβII	>10,000
CDK7/cyclin H	171	Hck	>10,000	PKCγ	>10,000
GSK3α	46	IGFR-1R	>10,000	PKCδ	>10,000
GSK3β	260	IKKα	>10,000	PKCε	>10,000
Abl (m)	>10,000	IKKβ	>10,000	PKCη	>10,000
Abl	>10,000	IR	>10,000	PKCι	>10,000
Abl (T315I)	>10,000	IRAK4	>10,000	PKCμ	>10,000
ALK	>10,000	JNKα1	>10,000	PKCθ	>10,000
AMPK (r)	>10,000	JNK2α2	>10,000	PKCζ	>10,000
Arg	>10,000	JNK3	>10,000	PKD2	>10,000
Arg (m)	>10,000	Lck	>10,000	Plk3	>10,000
ASK1	>10,000	Lyn	>10,000	PRAK	>10,000
Aurora-A	>10,000	Lyn (m)	>10,000	PRK2	>10,000
Axl	>10,000	MAPK1	>10,000	Ret	>10,000
Blk (m)	>10,000	MAPK2	>10,000	ROCK-I	>10,000
Bmx	>10,000	MAPKAP-K2	>10,000	ROCK-II	>10,000
BTK	>10,000	MAPKAP-K3	>10,000	Ron	>10,000
CaMKII (r)	>10,000	MEK1	>10,000	Ros	>10,000
CaMKIV	>10,000	Met	>10,000	Rse	>10,000
CHK1	>10,000	MKK4 (m)	>10,000	Rsk1	>10,000
CHK2	>10,000	MKK6	>10,000	Rsk1(r)	>10,000
CK1(y)	>10,000	MKK7β	>10,000	Rsk2	>10,000
CK1δ	8,270	MSK1	>10,000	Rsk3	>10,000
CK2	>10,000	MST2	>10,000	SAPK2a	>10,000

(*Continued on the following page*)

Table 1. Kinase activity of R547 (Cont'd)

B. Inhibitory activity of R547 in the Upstate kinase selectivity screen

Kinase	IC_{50} (nmol/L)	Kinase	IC_{50} (nmol/L)	Kinase	IC_{50} (nmol/L)
c-RAF	>10,000	NEK2	>10,000	SAPK2b	>10,000
CSK	>10,000	NEK6	>10,000	SAPK3	>10,000
cSRC	>10,000	NEK7	>10,000	SAPK4	>10,000
DDR2	>10,000	P70S6K	>10,000	SGK	>10,000
EGFR	>10,000	PAK2	>10,000	Syk	>10,000
EphA2	>10,000	PAK4	>10,000	TAK1	>10,000
EphB2	>10,000	PAR-1Bα	>10,000	Tie2	>10,000
EphB4	>10,000	PDGFRα	>10,000	TrkA	>10,000
ErbB4	>10,000	PDGFRβ	>10,000	TrkB	>10,000
Fes	>10,000	PDK1	>10,000	Yes	>10,000
Fgr	>10,000	Pim-1	>10,000	ZAP-70	>10,000
FGFR1	>10,000	P13Kγ	>10,000		

*$K_i = IC_{50} / (1 + S / K_m)$, where S is the substrate ATP concentration and K_m is the Michaelis-Menten constant for ATP; mean of at least two separate determinations.

test and one-way ANOVA and a post hoc Bonferroni t test (SigmaStat version 2.0, Jandel Scientific, San Francisco, CA). Differences between groups are considered significant when $P < 0.05$.

Pharmacokinetic Determination

In some studies, plasma and tumor samples were collected and analyzed for R547 by liquid chromatography-tandem mass spectrometry. Mean plasma concentrations were calculated from three animals per group per time point. Plasma samples with concentration below the limit of quantification (<12.5 ng/mL) were set to zero. Pharmacokinetic variables were estimated from the mean plasma concentration data. C_{max} values (maximum plasma concentration) were taken directly from the plasma concentration-time profiles at the first time point without any extrapolation, and the area under the plasma concentration versus time curve (AUC) was calculated using the linear trapezoidal rule. For the pharmacodynamic biomarker studies, individual tumors were collected from rats at specified times after dosing, snap frozen in liquid nitrogen, and stored at −80°C.

Results

R547 Is Selective for the CDK Family of Kinases

R547 is a potent ATP-competitive inhibitor of CDK1/cyclin B ($K_i = 2 \pm 0.8$ nmol/L), CDK2/cyclin E ($K_i = 3 \pm 0.8$ nmol/L), and CDK4/cyclin D ($K_i = 1 \pm 0.1$ nmol/L). The IC_{50} for inhibition of these CDKs at increasing ATP concentrations was linear relative to the ATP concentration present in the reaction, consistent with an ATP-competitive mode of inhibition. Inhibition of CDK4 activity relative to ATP by R547 is shown in Fig. 1B. R547 was >1,000-fold selective against our internal panel of 21 serine/threonine and tyrosine kinases (Table 1A). In the Upstate kinase selectivity screen, R547 showed ≥50% inhibition of only 10 of 122 kinases tested at 10 μmol/L (Table 1B). It was most active against the CDK family of kinases with potent activity (IC_{50}, ≤4 nmol/L) in the CDK1/cyclin B, CDK2/cyclin E, CDK2/cyclin A, CDK3/cyclin E, CDK5/p35, and CDK6/cyclin D3 assays. R547 strongly inhibited all five of these kinases and had intermediate activity against CDK7/cyclin H (IC_{50}, 171 nmol/L), GSK3α (IC_{50}, 46 nmol/L), and GSK3β (IC_{50}, 260 nmol/L). Most significantly, R547 was inactive against the other 113 kinases in the panel (IC_{50}, ≥8,200 nmol/L).

R547 Has Antiproliferative Activity in Tumor Cells Independent of p53, Retinoblastoma, or MDR Status

The *in vitro* antiproliferative effects of R547 were evaluated by the 3-(4,5-dimethylthiazol-2-yl)-2,5-diphenyltetrazolium bromide (MTT) tetrazolium dye assay in several human tumor cell lines that originated from breast, colon, lung, cervix, prostate, osteosarcoma, and melanoma tissues as well as B-cell lymphomas. The data indicate that R547 has potent *in vitro* antiproliferative activity (IC_{50}, ~0.05–0.6 μmol/L) independent of the tissue of origin, p53, or retinoblastoma status of the cells (Table 2A). R547 was also tested in tumor cells from two rodent species (data not shown). As with the human tumor cell lines, R547 was very effective in inhibiting the growth of the rat mammary cell line MTLn3 and the rat prostate cell line Mat-Lylu (IC_{50}, ≤0.2 μmol/L).

Several general mechanisms that play a role in clinical resistance to certain neoplastic agents are associated with well-known natural product anticancer agents [e.g., paclitaxel (Taxol) and doxorubicin/Adriamycin]. One of these phenomena is MDR, which can be mediated by P-glycoprotein-dependent or P-glycoprotein-independent mechanisms (37). The *in vitro* antiproliferative activity of R547 was not affected by P-glycoprotein overexpression in cells. The effect of R547 on the *in vitro* growth of KB-3-1, a non-MDR parental cell line, and the corresponding MDR KB-A-1 cells, shown to overexpress P-glycoprotein (28), was evaluated. Paclitaxel, a known P-glycoprotein

substrate (38), was included as a positive control, and 5-fluorouracil was included as a negative control. The IC_{50} of the compounds in the individual cell lines is presented in Table 2B along with calculated non-MDR/MDR ratios. Paclitaxel antiproliferative activity dramatically decreased in the MDR cell line compared with the parental non-MDR cell line (>294-fold). In contrast, R547 had comparable activity in both cell lines, and the activity did not seem to be modulated by P-glycoprotein overexpression.

R547 Blocks Tumor Cells in G_1 Plus G_2 and Induces Apoptosis

The cell cycle effects of R547 on HCT116 colon tumor cells are shown in Fig. 2A. Cells were treated for 20 hours with DMSO (control) or with 0.1, 0.2, and 0.6 μmol/L R547. These concentrations are equivalent to the IC_{50}, IC_{90}, and $3 \times IC_{90}$ of the compound as determined in the MTT assay. The cells were harvested and stained with propidium iodide for DNA content and BrdUrd for S phase content. Flow cytometry results show a dose-dependent decrease in BrdUrd incorporation and in percentage S phase in the presence of R547, indicative of a cell cycle block in G_1-S plus G_2-M. In the HCT116 DMSO-treated control cells, 30% of the cells were in S phase. After exposure to 0.6 μmol/L R547 for 20 hours, S phase decreased to ~8% of the cell population. A similar dose-dependent decrease in S phase was observed in H460a human lung cells, in DU145 human prostate, and in MDA-MB-468 human breast cell lines (data not shown) treated with R547.

There is a distinct class of proteins phosphorylated during the G_2-M transition. The MPM2 antibody specifically recognizes a phosphorylated epitope from that class and helps distinguish mitotic cells from interphase cells. HCT116 cells treated with R547 for 20 hours were double stained with propidium iodide for DNA content and with MPM2 for evidence of mitosis. Results are shown in Fig. 2B. The cytograms are gated to show the MPM2-stained cells in the upper right quadrant. Control samples treated with DMSO show few cells (3%) in the upper right quadrant.

Nocodazole, a known M phase inhibitor, resulted in 60% of the cells in this quadrant (data not shown), whereas cells treated with $3 \times IC_{90}$ of R547 had <0.5% cells in the upper right quadrant. Cells with 4 N DNA were blocked in the G_2 phase of the cell cycle as shown by the lack of MPM2 staining.

Tumor cells blocked in the cell cycle for extended periods frequently undergo apoptosis or programmed cell death, characterized by membrane blebbing and cell shrinkage followed by cell and nuclear disintegration

Table 2. Cell cytotoxicity of R547

A. Cell cytotoxicity in a 5-day MTT assay in human tumor cell lines treated with R547

Cell line	Origin	p53 status	Retinoblastoma status	IC_{50}* (μmol/L) ± SD
MDA-MB-468	Breast carcinoma	Mutant	Mutant	0.11 ± 0.01
MDA-MB-435	Breast carcinoma	Mutant	Wild-type	0.08 ± 0.01
MCF-7	Breast carcinoma	Wild-type	Wild-type	0.06 ± 0.01
HCT116	Colon carcinoma	Wild-type	Wild-type	0.08 ± 0.01
SW480	Colon carcinoma	Mutant	Wild-type	0.07
RKO	Colon carcinoma	Wild-type	Wild-type	0.05
HT-29	Colon carcinoma	Mutant	Wild-type	0.17
HCT15	Colon carcinoma	Mutant	Wild-type	0.61 ± 0.02
H460a	Lung carcinoma	Wild-type	Wild-type	0.06 ± 0.01
C33A	Cervical carcinoma	Mutant	Mutant	0.32 ± 0.04
DU145	Prostate carcinoma	Mutant	Mutant	0.08 ± 0.04
OSA-CL	Osteosarcoma	Mutant	Wild-type	0.19
LOX	Melanoma	Wild-type	Wild-type	0.05
JEKO-1	Mantle cell lymphoma	Mutant	Wild-type	0.08 ± 0.01
REC-1	Mantle cell lymphoma	Wild-type	Wild-type	0.09 ± 0.03

B. Cytotoxicity in a MDR and non-MDR cell line treated with R547, paclitaxel, and 5-fluorouracil

Cell line	R547, IC_{50} (μmol/L) ± SD	Paclitaxel, IC_{50} (μmol/L) ± SD	5-Fluorouracil, IC_{50} (μmol/L) ± SD
(Non-MDR) KB-3-1	0.11 ± 0.01	<0.005	4.32 ± 0.11
(MDR) KB-A-1	0.39 ± 0	1.47 ± 0	5.51 ± 0.36
IC_{50} (MDR)/IC_{50} (non-MDR)	3	>294	1

NOTE: Values are the concentrations of R547 necessary to inhibit proliferation by 50% and represent the average of at least two separate experiments done in duplicate. The activity of the compounds on the MDR cell line compared with the parental line was calculated by dividing the IC_{50} in the MDR cell line by the IC_{50} in the non-MDR cell line.

*IC_{50} is the concentration of drug necessary to inhibit cell proliferation by 50%.

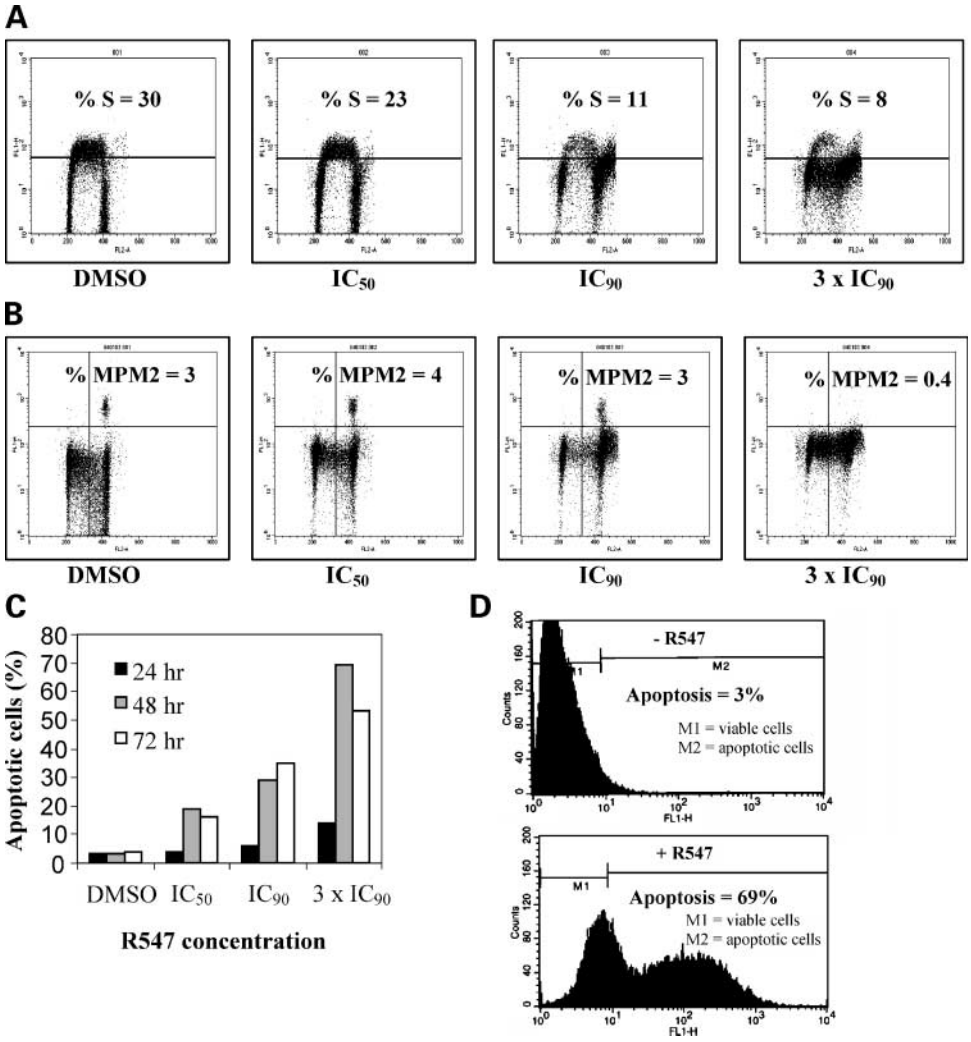

Figure 2. R547 induces a dose-dependent $G_1 + G_2$ cell cycle block followed by apoptosis in human tumor cells. Asynchronous HCT116 cells were exposed to either DMSO or R547 for 20 h. **A,** cells were analyzed for ability to incorporate BrdUrd into DNA. *Top quadrant,* cells that are progressing through S phase. **B,** cells were assayed for cell cycle distribution as measured by propidium iodide and MPM2 staining. *Top right quadrant,* cells that are in M phase. **C,** cells were exposed to either DMSO or R547 and harvested 24, 48, and 72 h after treatment. The percentage apoptotic cells were determined using the APO-BRDU assay kit. The data shown are a representative data set done as singlets. **D,** HCT116 cells were exposed to either DMSO (*top*) or R547 at 3 × IC_{90} obtained in the MTT proliferation assay (*bottom*). Cells were harvested after 48 h, and the percentage apoptotic cells were determined using the APO-BRDU assay kit. The region marked M2 was used to quantify the number of apoptotic cells.

and intranucleosomal DNA fragmentation. One of the hallmarks of apoptotic cells is accumulation of DNA strand breaks. To examine the effects of treatment with R547 on DNA fragmentation, cells treated with compound were evaluated using the APO-BRDU assay kit, which labels DNA breaks and total cellular DNA and allows for the detection and quantification of nonapoptotic and apoptotic cells by flow cytometry. For these studies, HCT116 cells were treated with DMSO or compound for 24 to 72 hours and then processed as described in Materials and Methods. The percentage apoptotic cells from each of the treatment groups are shown in Fig. 2C, and the DNA fragmentation profile of cells treated with either DMSO or R547 for 48 hours is compared in Fig. 2D. In the DMSO-treated cells, the majority of the cells (97%) were viable and did not contain DNA strand breaks. These are the cells located in the M1 region of the histogram. Treatment with R547 at 3 × IC_{90} for 48 hours resulted in shift of the fluorescence profile to the right as a result of increased BrdUTP incorporation. Approximately 69% of the cells shift into the M2 region and are apoptotic. These data confirm that R547 induces apoptosis as measured by DNA fragmentation.

R547 Inhibits Phosphorylation of Retinoblastoma Protein in Human Tumor Cells

HCT116 cells were treated for 20 hours at the IC_{50} (0.1 μmol/L), IC_{90} (0.2 μmol/L), and 3 × IC_{90} (0.6 μmol/L) concentration for cell growth inhibition, and lysates were analyzed by Western blotting for retinoblastoma phosphorylation at the Ser^{795} and Ser^{780} sites (Fig. 3A). Treatment with R547 resulted in inhibition of phosphorylation at both CDK phosphorylation sites in a concentration-dependent fashion. HCT116 cells treated for 24, 48, and 72 hours with R547 also showed a band corresponding to a p48/retinoblastoma fragment that becomes more intense at 48 and 72 hours after treatment with R547 (Fig. 3B). Caspase-mediated interior cleavage of retinoblastoma protein, resulting in the generation of a p48 and a p68 retinoblastoma fragment, has been reported at the onset of apoptosis (39, 40). The appearance of this p48/retinoblastoma fragment is consistent with the inhibition of retinoblastoma protein phosphorylation at 24 hours and the induction of apoptosis 48 hours after treatment with R547.

R547 similarly affected the phosphorylation status of JEKO-1, a human B-cell lymphoma cell line. JEKO-1 cells

were treated for 20 hours at the IC_{50} (0.08 μmol/L), IC_{90} (0. 20 μmol/L), and 3 × IC_{90} (0.60 μmol/L) concentrations for cell growth inhibition. Lysates were analyzed by Western blotting for retinoblastoma phosphorylation at Thr^{821}. Treatment with R547 resulted in dose-dependent inhibition of retinoblastoma phosphorylation (Fig. 3C).

R547 Has Significant *In vivo* Efficacy with Daily Oral and Once Weekly i.v. Dosing

R547 showed antitumor activity in all of the models tested to date, including six human tumor xenografts and an orthotopic syngeneic rat model. Statistically significant antitumor activity ($P < 0.01$) was observed after oral and i.v. dosing of R547 in multiple established human tumor xenograft models (Table 3). R547 showed significant TGI (79–99%) in colon, lung, breast, prostate, and melanoma human tumor xenograft models with 40 mg/kg daily oral dosing. R547 was equally efficacious (TGI, 61–95%) when dosed with 40 mg/kg i.v. once weekly. These doses were not toxic and did not result in body weight loss. The animals did not show signs of overt toxicity during the course of the 3-week study nor was there any gross pathology observed at necropsies done at the end of the studies.

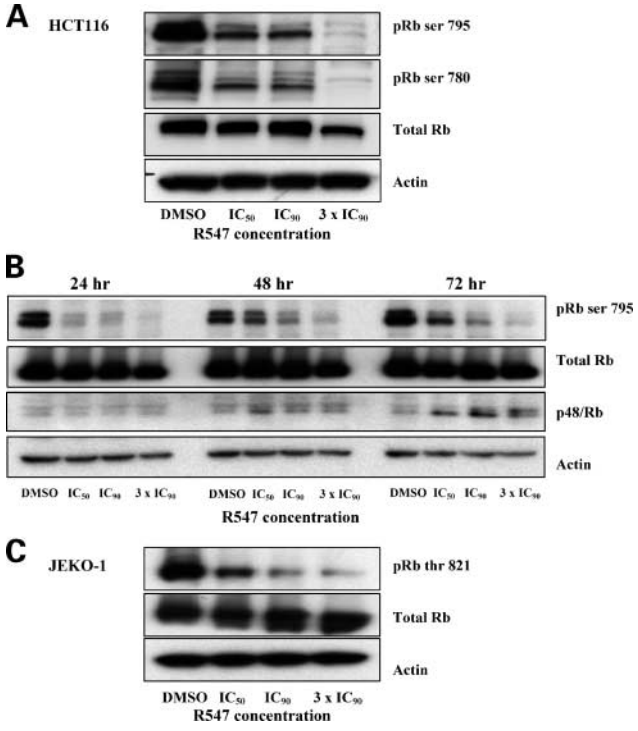

Figure 3. R547 inhibits retinoblastoma protein phosphorylation in human tumor cells. **A,** HCT116 cells were treated with DMSO or R547 at the indicated concentrations for 20 h. Cell lysates were prepared, and protein was resolved by SDS-PAGE and subjected to Western blotting of the stated proteins relative to the DMSO control. **B,** HCT116 cells were treated with DMSO or R547 at the indicated concentrations for 24, 48, and 72 h. Cell lysates were prepared, and protein was resolved by SDS-PAGE and subjected to Western blotting of the stated proteins relative to the DMSO control. **C,** JEKO-1 tumor cells were treated with DMSO or R547 at the indicated concentrations for 20 h after which cell lysates were prepared and protein was resolved by SDS-PAGE and subjected to Western blotting of the indicated protein.

TGI by R547 seemed to be less dependent on the schedule of administration and more dependent on the cumulative weekly dose. In the HCT116 human colon model, R547 showed 91% TGI with daily oral dosing using 40 mg/kg (Fig. 4A). Antitumor activity was further evaluated in this model using different doses and schedules of administration. The same total daily dose of R547 administered as a single dose (38 mg/kg qd), or given twice daily (19 mg/kg bd) or thrice daily (12.5 mg/kg tid) over a 3-week period, showed comparable TGI ranging from 71% to 90% (Fig. 4B). Further, the same total weekly dose administered as a single dose (300 mg/kg q7d) showed comparable TGI of 92% (Fig. 4C). Equivalent antitumor efficacy was observed after i.v. once weekly dosing with 40 and 60 mg/kg (Fig. 4D).

R547 was also evaluated in a rat syngeneic tumor model using the once weekly dosing regimen and showed significant TGI (≥84%) when administered once weekly by the oral and the i.v. route. In the MTLn3 rat mammary tumor model, R547 was active when dosed orally at 80 mg/kg once weekly (Fig. 5A) and equally active at 15 and 30 mg/kg administered i.v. once weekly (Fig. 5C).

Pharmacokinetic samples were taken at the end of some of the efficacy studies to assess compound exposures. In both the human tumor xenograft and the syngeneic rat models, the total weekly exposure (AUC/wk) of R547 seems to be driving efficacy (Table 4A). An AUC/wk of ≥12,000 ng hr/mL resulted in significant TGI independent of dosing regimen or route of administration. In these studies, the C_{max} ranged from 474 to 27,000 ng/mL and did not seem to directly contribute to the efficacy of R547. In the MTLn3 rat model, dosed i.v. once weekly (q7d) at 7.5 mg/kg, an AUC/wk of ~6,000 ng hr/mL was not efficacious despite a high C_{max}, whereas 15 mg/kg q7d, with an AUC/wk of 17,300 ng hr/mL, was highly efficacious (Table 4B). Clinical studies will be needed to accurately define the dose-exposure-efficacy relationship, but preclinical data suggest that an AUC/wk of ≥20,000 ng hr/mL is needed to achieve efficacy.

R547 Is Measurable in Tumor Tissue after Oral and i.v. Dosing

Pharmacokinetic samples were taken at the end of the MTLn3 rat tumor studies, and the concentrations of R547 were determined in both the plasma and the corresponding tumor tissue. A high ratio of tumor to plasma levels of drug was observed. After a single oral dose of 80 mg/kg, plasma and tumor tissues show a similar concentration time profile of R547 (Fig. 5B). Maximum concentrations in both plasma and tumor tissue were observed 1 hour after dose, and tumor drug concentrations were ~50% of the plasma concentration. Drug levels in plasma and tumor tissues were measurable up to 24 hours after dosing, and at 24 hours, tumor drug levels (164 ± 28 ng/g) approximated plasma exposures (250 ± 74 ng/mL). Exposures over the entire dosing interval were greater than concentrations that inhibited the growth of the tumor cells in culture (IC_{50}, 0.17 μmol/L). Only one of three animals had measurable plasma drug levels (≥12.5 ng/mL) 72 hours after dosing. In general, plasma drug concentration data seem to reflect tumor concentrations.

Table 3. *In vivo* efficacy with oral and i.v. dosing of R547 in established human tumor models

Tumor model (source)	TGI (%),* 40 mg/kg once daily oral dosing	Final mean tumor volume ± SD (mm^3)		TGI (%),* 40 mg/kg once weekly i.v. dosing	Final mean tumor volume ± SD (mm^3)	
		Vehicle	R547		Vehicle	R547
HCT 116 (colon)	91	1,658 ± 334.09	229.8 ± 72.0†	88	1,292.24 ± 426.01	240.50 ± 98.02†
H460a (lung)	80	1,053.0 ± 545.6	268.78 ± 118.01†	61	1,674.43 ± 693.15	738.12 ± 375.92†
MDA-MB-435 (breast)	79	509.38 ± 175.21	220.23 ± 39.25†	78	509.38 ± 175.21	229.02 ± 50.63†
DU145 (prostate)	85	623.11 ± 139.27	184.34 ± 68.41†	95	365.76 ± 223.85	122.67 ± 49.17†
A549 (lung)	98	920.57 ± 221.02	133.66 ± 55.49†	92	920.57 ± 221.02	180.82 ± 59.38†
LOX (melanoma)	99	2,568.4 ± 1,211	117.39 ± 37.70†	ND	ND	ND

Abbreviation: ND, not determined.
*Percentage change in tumor volume is calculated using the following formula: $[(T - T_0) / T_0] \times 100$, where '$T$' represents mean tumor volume of the treated group at a particular day and 'T_0' represents mean tumor volume of the same treated group at initiation of treatment.
†$P < 0.01$.

Similarly, a single 25 mg/kg i.v. dose of R547 was administered to female Fischer rats bearing MTLn3 tumors (Fig. 5D), and plasma and tumor samples were analyzed for drug. R547 levels were measurable up to 6 hours in plasma and up to 24 hours in the tumor tissue, indicating a longer elimination half-life in the orthotopically implanted rat tumors. The R547 concentrations in tumors 16 hours after dose were equivalent to the IC_{50} concentration of R547 determined in the MTLn3 tumor cell proliferation assay.

R547 Inhibits Phosphorylation of Retinoblastoma Protein in Tumors

The retinoblastoma phosphorylation status in tumor tissue was monitored over time. Treatment of female Fischer rats bearing MTLn3 tumors with a single oral efficacious dose of 80 mg/kg R547 resulted in a reduction in phosphorylation of retinoblastoma in the tumors up to 6 hours after dosing (Fig. 6A). Each of the lanes represents a tumor isolated from one animal, and for each time point, three different tumors were analyzed, with similar decreases in phosphorylated retinoblastoma observed. The retinoblastoma protein Ser^{807}/Ser^{811} antibody was used for detection of retinoblastoma protein in these immunoblotting experiments as it gave the strongest signal in blots where tumor lysates were evaluated. Total retinoblastoma levels did not seem altered by treatment. A similar decrease in retinoblastoma protein after dosing was also seen by immunohistochemistry (data not shown) in the LOX melanoma xenograft model after dosing.

Treatment of female Fischer rats bearing MTLn3 tumors with a single efficacious i.v. dose of 25 mg/kg also results in reduced retinoblastoma phosphorylation in tumors. Phosphorylated retinoblastoma in tumor lysates was measured using retinoblastoma protein Ser^{807}/Ser^{811} and retinoblastoma protein Ser^{795} antibodies. Phosphorylation at Ser^{807}/Ser^{811} was not detected at any of the time points after dosing, and phosphorylation at Ser^{795} was reduced at 4 hours after dosing and totally inhibited at 16 and 24 hours after dosing (Fig. 6B). Total retinoblastoma also decreased and was not detected at the later time points. The degradation of retinoblastoma protein is consistent with the apoptotic effect of the compound on cells and a direct result of the interior cleavage of the retinoblastoma protein that reportedly occurs during apoptosis (40). Evaluation of apoptosis in the tumor tissue is planned and may help egplain the efficacy seen with the once weekly i.v. dosing regimens.

Various *ex vivo* pharmacodynamic assays based on CDK inhibition have been proposed (41). The availability of a surrogate tissue, such as skin or peripheral blood mononuclear cells (PBMC), or use of a biological fluid, such as urine, to monitor pharmacodynamic effects to eliminate the need for tumor biopsies is highly desirable but thus far has proved to be difficult. The use of PBMCs, which are not cycling cells, is a special challenge as cells require *ex vivo* stimulation (42, 43). In addition, protocols for isolation of PBMCs require manipulation, resulting in loss of the drug and observations of no effect either on the cell cycle or on phosphorylated retinoblastoma, as seems to be the case with flavopiridol (44, 45). We, however, did see an effect on phosphorylated retinoblastoma in *ex vivo* mitogen-stimulated PBMCs isolated from animals treated *in vivo* with efficacious doses of R547 (data not shown). Although the binding of R547 to the CDK enzymes is reversible, the measured dissociation constant of <0.1 per hour (data not shown) is low, and R547 may be retained during the PBMC isolation step. This is being further investigated, as PBMCs would provide an accessible surrogate tissue for monitoring CDK inhibition.

Discussion

The deregulation of CDK activity in cancer has driven the development of small-molecule inhibitors of CDKs for the treatment of this disease with several targeted CDK inhibitors entering the clinic (45, 46). This therapeutic strategy is complicated by the fact that several CDKs have cellular roles not related to the cell cycle. In addition, new

evidence that some CDKs believed to be essential for cell cycle progression may in fact be dispensable has made the choice of a specific CDK target more challenging, and there are several CDK inhibitors in preclinical development now focusing on inhibiting more than a single CDK or kinase target (8, 26).

In this report, we describe R547, a potent and multi-targeted CDK selective inhibitor. R547 showed the greatest activity against the CDKs involved in cell cycle control and against CDK5 (IC_{50}s, ≤4 nmol/L) and intermediate activity against CDK7, GSK3α, and GSK3β (IC_{50}s, 46–260 nmol/L). The GSK3 kinases are phylogenetically most closely related to the CDKs, and consequently, most CDK inhibitors are also good inhibitors of GSK3β due to the similarity of the ATP-binding domain in the GSK family (47). In contrast, R547 was markedly more potent toward the CDK family than it was to the GSK3 family and, more importantly, was not active against the other 113 kinases in the panel (IC_{50}s, >8,000 nmol/L).

R547 had potent antiproliferative activity (IC_{50}, ≤0.6 μmol/L) in 19 of 19 cell lines tested irrespective of tissue of origin, p53, MDR, or retinoblastoma status. Treatment of tumor cell lines with R547 caused a dose-dependent cell cycle block in G_1 and G_2-M boundaries with the greatest effect seen 24 hours after treatment. Further analysis with a mitotic specific monoclonal antibody (MPM2) confirmed that the cells are blocked in G_2. The ability of R547 to induce apoptosis was also examined. Approximately 69% of the cells treated with R547 undergo apoptosis within 48 hours of drug treatment. The time course of appearance of the DNA strand breaks is consistent with our hypothesis that the cells undergo G_1 and G_2 arrest followed 24 hours later by apoptosis. These data indicate that the *in vitro* antiproliferative activities of R547 are mediated by its ability to inhibit cell cycle progression, arrest cells in G_1 plus G_2, and subsequently induce apoptosis.

We also showed that R547 inhibits phosphorylation of the retinoblastoma protein at putative CDK phosphorylation

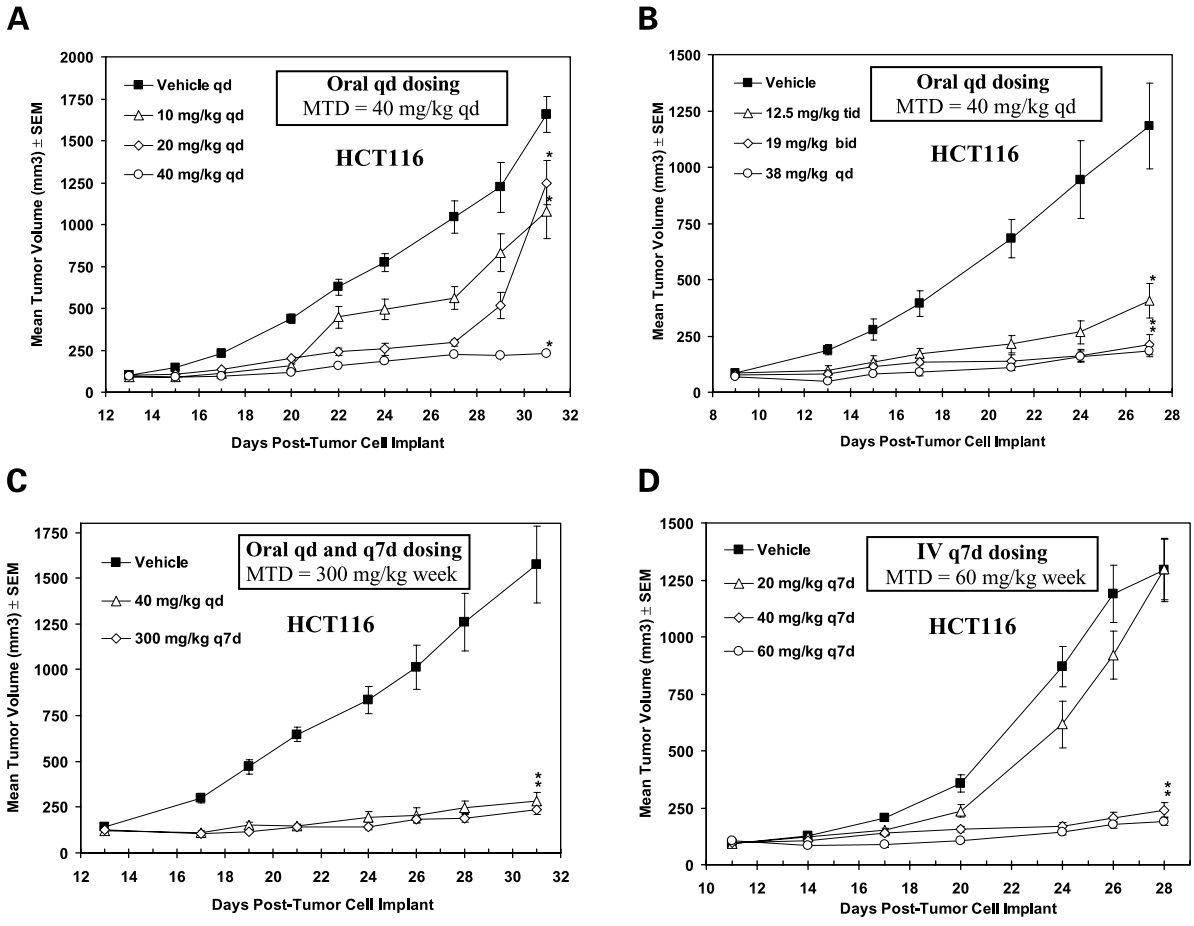

Figure 4. R547 has *in vivo* antitumor activity using both daily oral and once weekly i.v. dosing regimens. HCT116 tumor cells were implanted s.c. in the right flank of female nude mice and allowed to grow to a least 100 mm^3 before start of dosing. R547 was dosed for 18 d. **A,** R547 was given orally once daily by gavage at the indicated drug doses. **B,** R547 was administered orally at the previously determined efficacious dose of 38 mg/kg. The 38 mg/kg dose was administered as a single dose, 19 mg/kg dosed 12 h apart or 12.5 mg/kg dosed 8 h apart. **C,** R547 was dosed orally once daily at 40 mg/kg and once weekly at 300 mg/kg. **D,** cells were implanted into nude mice as described above, and R547 was administered i.v. once weekly by tail vein injection at the indicated doses. Data are shown starting from the first day of dosing. *, *P*s < 0.05.

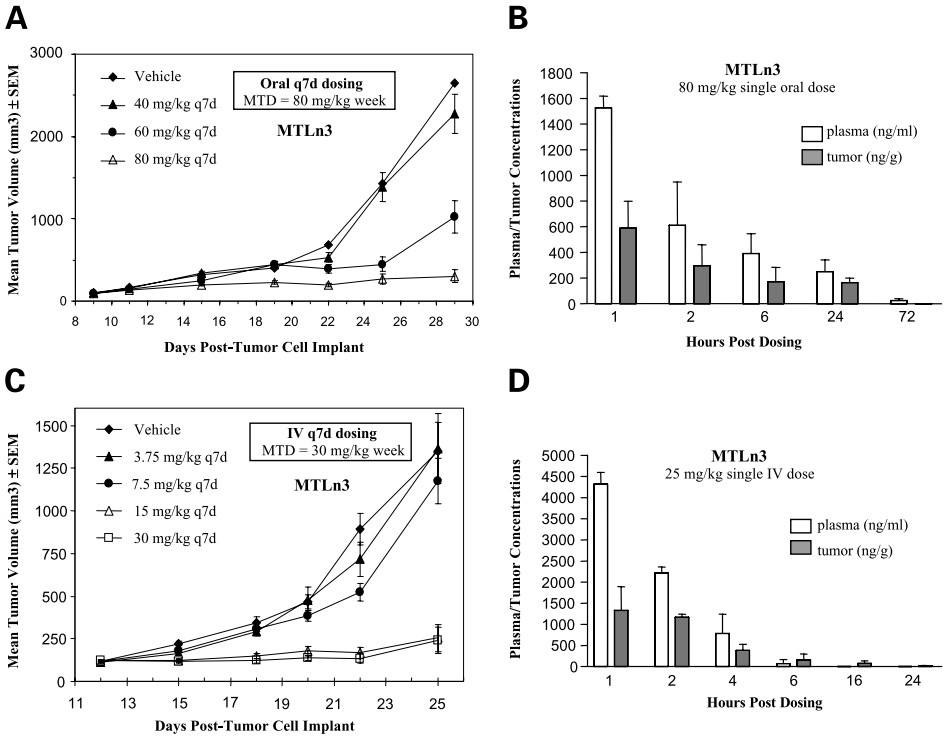

Figure 5. R547 has *in vivo* antitumor activity by both the oral and i.v. route of administration. **A,** MTLn3 rat mammary tumor cells were implanted in the mammary fat pad of female Fischer rats and allowed to grow to at least 100 mm^3. R547 was administered orally once weekly at the indicated concentrations. **B,** a single 80 mg/kg dose of R547 was given orally to female Fischer rats bearing MTLn3 tumors. At the designated times after dosing, plasma and tumors were collected and plasma and tumor concentrations were determined. **C,** female Fischer rats bearing MTLn3 tumors were treated once weekly i.v. with R547 for a 2-wk period at the indicated doses. **D,** a single 25 mg/kg dose of R547 was given i.v. to female Fischer rats bearing MTLn3 tumors. Plasma and tumor samples were collected at the designated time points, and R547 concentrations were determined.

sites (48) in a concentration-dependent manner in cell lines. The effects on the Ser^{795}, Ser^{780}, Ser^{807}/Ser^{811}, and Thr^{821} phosphorylation sites occur at pharmacologically relevant exposures (IC_{50} to 3 × IC_{90}). R547 is a broad-spectrum CDK inhibitor; therefore, the effect on multiple retinoblastoma protein sites is as expected. Because retinoblastoma is a direct substrate of the CDKs, the mechanism for the decrease in retinoblastoma phosphorylation is consistent with the inhibition of CDK by the compound in cells. However, multiple mechanisms can lead to reduced retinoblastoma protein phosphorylation, which leaves the possibility that additional or alternative modes of action of R547 in cells contribute to its activity. The effects of R547 on protein expression changes of key cell cycle regulatory proteins are being investigated.

When administered orally, R547 led to dose-dependent antitumor activity in several human tumor xenograft models. Promising activity in a rat syngeneic mammary tumor model was also observed. R547 was equally active when administered daily by the oral route or i.v. once weekly and showed significant TGI (≥61%) in five of five established tumor models at doses that did not result in body weight loss or overt toxicity. The dose-exposure-effect relationship observed indicates that C_{max} is not a likely pharmacokinetic driver of R547-mediated TGI in our tumor models. The data suggest that antitumor efficacy can be achieved with a high dose administered over a short period or with more frequent administration of a lower dose provided overall plasma exposures (AUC/wk) reach the efficacious threshold. Assessment of tissue drug levels shows that R547 gets into the tumor tissue after both oral and i.v. dosing, and concentrations equivalent to 0.6 μmol/L or ~2 × IC_{90} were detected in the tumors 24 hours after oral single dose administration and 6 hours after administration of a single i.v. dose of R547. These doses were shown to be efficacious in the rat tumor models.

We have also shown that R547 inhibits retinoblastoma protein in tumor cells and xenografts at multiple putative CDK phosphorylation sites. After administration of a single oral efficacious dose of R547, there was a clear inhibition of retinoblastoma phosphorylation up to 6 hours compared with the vehicle control in the MTLn3 rat tumors. After administration of a single i.v. efficacious dose of R547 in the same tumor model, phosphorylation of retinoblastoma protein was inhibited up to 24 hours after dosing in the tumors. Total retinoblastoma was also not detected in these samples at 16 and 24 hours, and the decrease in retinoblastoma protein is likely due to induction of apoptosis at the higher R547 plasma concentrations and the result of caspase-dependent cleavage of retinoblastoma. These data suggest that significant induction of apoptosis may be occurring following the higher single dose and are consistent with observed TGI with a once weekly dosing in the absence of a constant exposure to drug. The Ser^{807}/Ser^{811} site is reported to be phosphorylated by CDK4/cyclin D1, whereas the Ser^{795} site is phosphorylated by CDK2/cyclin A and CDK2/cyclin E (48). Interestingly, loss of phosphorylation at Ser^{807}/Ser^{811} occurred at 1 hour after dosing and preceded the loss of phosphorylation at Ser^{795}.

Table 4. R547 exposures for efficacy

A. R547 exposures for efficacy in established tumor models

Tumor model	Dose (mg/kg)	Dosing route and schedule	C_{max}* (ng/mL)	AUC/wk* (ng hr/mL)	TGI (%)†
HCT116 (human)	30	I.v. 1 × week	27,000	18,800	91
HCT116 (human)	40	Oral daily	869	19,537	91
MTLn3 (rat)	15	I.v. 1 × week	13,100	17,300	89
MTLn3 (rat)	80	Oral 1 × week	474	12,000	92

B. AUC vs C_{max} exposures in MTLn3 rat model with q7d i.v. dosing

Dose (mg/kg)	C_{max}* (ng/mL)	AUC/wk* (ng hr/mL)	TGI (%)†
3.75	6,840	2,260	No efficacy
7.5	10,900	5,730	No efficacy
15	13,100	17,300	89
30	70,100	56,700	90

*Values calculated from end of efficacy study pharmacokinetic samples (n = 3).
†Percentage change in tumor volume is calculated using the following formula: $[(T - T_0) / T_0] \times 100$, where '$T$' represents mean tumor volume of the treated group at a particular day and 'T_0' represents mean tumor volume of the same treated group at initiation of treatment.

Because R547 inhibits both kinases equipotently in cells and the tumor cells are not synchronized, the significance of the earlier effect on Ser^{807}/Ser^{811} phosphorylation cannot be fully explained.

Recent data indicate that cells can recover from targeted inhibition of a single CDK by compensatory activity from other CDKs. It is therefore speculated that a potent and multitargeted CDK inhibitor could eliminate this compensatory activity and should display robust cell cycle–mediated antiproliferative activity. We have identified such a compound. R547 is a potent and highly selective CDK inhibitor that has shown a breadth of activity *in vitro* and *in vivo* with a mechanism of action consistent with inhibition of CDK activity and the ability to induce apoptosis. The efficacy of many anticancer compounds depends on their ability to induce apoptotic cell death, and modulation of this variable by R547 is an important contributor to its antiproliferative effects *in vitro* and likely *in vivo*.

Several CDK inhibitors are currently in preclinical development, the most advanced of these being flavopiridol and Seliciclib. For flavopiridol, novel drug schedules are necessary to overcome pharmacokinetic barriers and higher than expected concentrations of drug may be required *in vivo* due to high plasma protein binding (49). As a consequence of its oral bioavailability, clinical trials with flavopiridol have only investigated i.v. administration. Seliciclib, on the other hand, reportedly has good oral bioavailability, and twice daily dosing is being investigated in the clinic. Preclinical pharmacology studies indicated that extended exposure of tumors to Seliciclib is required for efficacy (50). The pharmacokinetic profile of R547 has enabled the compound to be dosed in preclinical models to effective concentrations by both i.v. and oral routes. R547 has shown a great flexibility in dosing and was active by the oral and i.v. routes using daily as well as intermittent dosing regimens. Other CDK inhibitors in clinical development have not reported such dosing flexibility either preclinically or clinically.

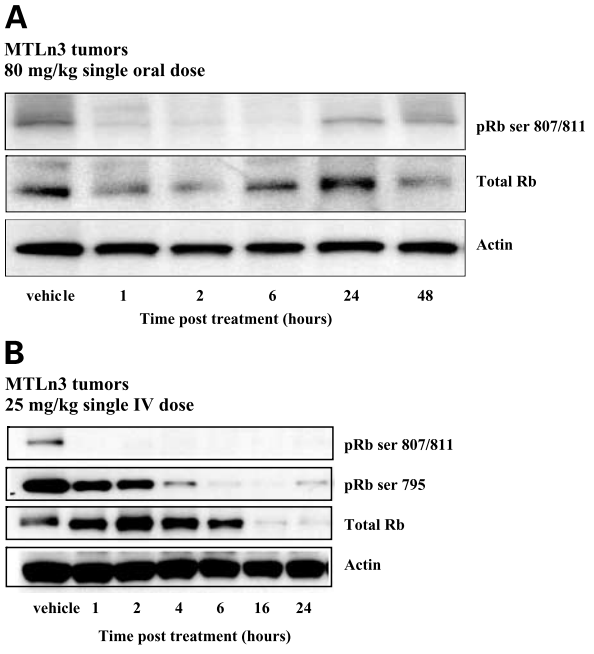

Figure 6. R547 inhibits retinoblastoma protein phosphorylation in tumors. **A,** tumors from female Fisher rats dosed orally with a single 80 mg/kg dose of R547 were removed at the indicated time points. Lysates were prepared and analyzed by Western blotting. **B,** tumors were isolated from female Fischer rats dosed i.v. with a single 25 mg/kg dose of R547 at the indicated time points. Tumor lysates were prepared, and protein was resolved by SDS-PAGE and subjected to Western blotting of the stated proteins relative to the vehicle control.

R547 seems to represent one of the most CDK potent and CDK selective compounds entering the clinic based on published studies (50, 51). R547 is currently in multicenter phase I clinical trials, and retinoblastoma protein phosphorylation is being used to monitor R547-related target modulation in patients.

Acknowledgments

We thank Drs. Mary Simcox and John Boylan for their critical reading of the article.

References

1. Sherr CJ. Cancer cell cycles. Science 1996;274:1672 – 7.

2. Harper JW, Adams PD. Cyclin-dependent kinases. Chem Rev 2001; 101:2511 – 26.

3. Pines J. Cyclins: wheels within wheels. Cell Growth Differ 1991;2: 305 – 10.

4. Maclachlan TK, Sang N, Giordano A. Cyclins, cyclin-dependent kinases, and cdk inhibitors: implications in cell cycle control and cancer. Crit Rev Eukaryot Gene Expr 1995;5:127 – 56.

5. Senderowicz AM, Sausville EA. Preclinical and clinical development of cyclin-dependent kinase modulators. J Natl Cancer Inst 2000;92: 376 – 87.

6. Knockaert M, Greengard P, Meijer L. Pharmacological inhibitors of cyclin-dependent kinases. Trends Pharmacol Sci 2002;23:417 – 25.

7. Benson C, Kaye S, Workman P, Garrett M, Walton M, de Bono J. Clinical anticancer drug development: targeting the cyclin-dependent kinases. Br J Cancer 2005;92:7 – 12.

8. Emanuel S, Rugg CA, Gruniger RH, et al. The *in vitro* and *in vivo* effects of JNJ-7706621: a dual inhibitor of cyclin-dependent kinases and aurora kinases. Cancer Res 2005;65:9038 – 46.

9. McClue SJ, Blake D, Clarke R, et al. *In vitro* and *in vivo* antitumor properties of the cyclin dependent kinase inhibitor CYC202 (R-Roscovitine). Int J Cancer 2002;102:463 – 8.

10. Fry DW, Harvey PJ, Keller PR, et al. Specific inhibition of cyclin-dependent kinase 4/6 by PD 0332991 and associated antitumor activity in human tumor xenografts. Mol Cancer Ther 2004;11:1427 – 38.

11. Misra RN, Xiao H, Kim KS, et al. *N*-(cycloalkylamino)acyl-2-aminothiazole inhibitors of cyclin-dependent kinase 2. *N*-[5-[[[5-(1,1-dimethylethyl)-2-oxazoyl]methyl]thio]-2-thiazolyl]-4-piperidinecarboxamide (BMS-387032), a highly efficacious and selective antitumor agent. J Med Chem 2004;47:1719 – 28.

12. Fry DW, Garrett MD. Inhibitors of cyclin-dependent kinases as therapeutic agents for the treatment of cancer. Curr Opin Oncol Endocr Metabol Invest Drugs 2000;2:40 – 59.

13. Garrett MD, Fattaey A. CDK inhibition and cancer therapy. Curr Opin Genet Dev 1999;9:104 – 11.

14. Meyer CA, Jacobs HW, Datar SA, Du W, Edgar BA, Lehner CF. *Drosophila* Cdk4 is required for normal growth and is dispensable for cell cycle progression. EMBO J 2000;19:4533 – 42.

15. Malumbres M, Hunt SL, Sotillo R, et al. Driving the cell cycle to cancer. Adv Exp Med Biol 2003;532:1 – 11.

16. Tetsu O, McCormick F. Proliferation of cancer cells despite CDK2 inhibition. Cancer Cell 2003;3:233 – 45.

17. Otega SO, Prieto I, Odajima J, et al. Cyclin-dependent kinase 2 is essential for meiosis but not for mitotic cell division in mice. Nat Genet 2003;35:25 – 31.

18. Chen YN, Sharma SK, Ramsey TM, et al. Selective killing of transformed cells by cyclin/cyclin-dependent kinase 2 antagonists. Proc Natl Acad Sci U S A 1999;96:4325 – 9.

19. Mendoza N, Fong S, Marsters J, Koeppen H, Schwall R, Wickramasinghe D. Selective cyclin-dependent kinase 2/cyclin A antagonists that differ from ATP site inhibitors block tumor growth. Cancer Res 2003;63:1020 – 4.

20. Ruetz S, Fabbro D, Zimmermann J, Meyer T, Gray N. Chemical and biological profile of dual Cdk1 and Cdk2 inhibitors. Curr Med Chem Anticancer Agents 2003;3:1 – 14.

21. Bashir T, Pagano M. Cdk1: the dominant sibling of Cdk2. Nat Cell Biol 2005;7:779 – 81.

22. Aleem E, Kiyokawa H, Kaldis P. Cdc2-cyclin E complexes regulate the G_1/S phase transition. Nat Cell Biol 2005;7:831 – 6.

23. Paglni G, Caceres A. The role of Cdk5-35 kinase in neuronal development. Eur J Biochem 2001;268:1528 – 33.

24. Gao C, Negash S, Guo HT, Ledee D, Wang H-S, Zelenka P. CDK5 regulates cell adhesion and migration in corneal epithelial cell. Mol Cancer Res 2002;1:12 – 24.

25. MacCallum DE, Melville J, Frame S, et al. Seliciclib (CYC202, R-Roscovitine) induces cell death in multiple myeloma cells by inhibition of RNA polymerase II-dependent transcription and down-regulation of Mcl-1. Cancer Res 2005;65:5399 – 407.

26. Cai D, Byth CIF, Shapiro GI. AZ703, an imidazo[1,2-*a*]pyridine inhibitor of cyclin-dependent kinases 1 and 2, induces E2F-1-dependent apoptosis enhanced by depletion of cyclin-dependent kinase 9. Cancer Res 2006;66:435 – 44.

27. Burgess A, Wigan M, Giles N, DePinto W, Stevens F, Gabrielli B. Inhibition of S/G_2 phase cdk4 reduces mitotic fidelity. J Biol Chem 2006; 281:9987 – 95.

28. Dolci ED, Abramson R, Xuan Y, et al. Anomalous expression of P-glycoprotein in highly drug resistant human KB cells. Int J Cancer 1993; 54:302 – 8.

29. Leibovitz A, Stinson JC, McCombs WB, III, McCoy CE, Maxur K, Marby N. Classification of human colorectal adenocarcinoma cell lines. Cancer Res 1976;36:4562 – 9.

30. Price JE. Metastasis from human breast cancer cell lines. Breast Cancer Res Treat 1996;39:93 – 102.

31. Neri A, Welch D, Kawaguchi T, Nicholson GL. Development of biologic properties of malignant cell sublines and clones of spontaneously metastasizing rat mammary adenocarcinoma. J Natl Cancer Inst 1982;68: 507 – 17.

32. Mukhopadhyay T, Tainsky M, Cavender AC, Roth JA. Specific inhibition of K-ras expression and tumorigenicity of lung cancer cells by antisense RNA. Cancer Res 1991;51:1744 – 8.

33. Denizot F, Lang R. Rapid colorimetric assay for cell growth and survival. Modifications to the tetrazolium dye procedure giving improved sensitivity and reliability. J Immunol Methods 1986;89:271 – 7.

34. Dermatakis A, Luk K-C, DePinto W. Synthesis of potent oxindole CDK2 inhibitors. Bioorg Med Chem 2003;11:1873 – 81.

35. Bussink J, Terry NHA, Brock WA. Cell cycle analysis of synchronized Chinese hamster cells using bromodeoxyuridine labeling and flow cytometry. In Vitro Cell Dev Biol Anim 1995;31:547 – 52.

36. Andreassen PR, Margolis RL. Microtubule dependency of $p34^{cdc2}$ inactivation and mitotic exit in mammalian cell. J Cell Biol 1994;127: 789 – 802.

37. Agus DB, Cordon-Cardo C, Fox W, et al. Prostate cancer cell cycle regulators: response to androgen withdrawal and development of androgen independence. J Natl Cancer Inst 1999;91:1869 – 76.

38. Beck WT, Qian XD. Photoaffinity substrates for P-glycoprotein. Biochem Pharmacol 1992;43:89 – 93.

39. An B, Dou QP. Cleavage of retinoblastoma protein during apoptosis: an interleukin 1β-converting enzyme-like protease as candidate. Cancer Res 1996;56:438 – 42.

40. Fattman CL, An B, Dou QP. Characterization of interior cleavage of retinoblastoma protein in apoptosis. J Cell Biochem 1997;67: 399 – 408.

41. Alzani R, et al. *Ex vivo* analysis to study the mode of action of a CDK2 inhibitor. Proc Am Assoc Cancer Res 2002;43:329.

42. Furukawa Y, DeCaprio JA, Freedman A, et al. Expression and state of phosphorylation of the retinoblastoma susceptibility gene product in cycling and noncycling human hematopoietic cells. Proc Natl Acad Sci U S A 1990;87:2770 – 4.

43. Juan G, Gruenwald S, Darzynkiewicz Z. Phosphorylation of retinoblastoma susceptibility gene protein assayed in individual lymphocytes during their mitogenic stimulation. Exp Cell Res 1998;239:104 – 10.

44. Shapiro GI. Preclinical and clinical development of the cyclin-dependent kinase inhibitor flavopiridol. Clin Cancer Res 2004;10: 4270 – 5S.

45. Stadler WM, Vogelzang NJ, Amato R, et al. Flavopiridol, a novel

cyclin-dependent kinase inhibitor, in metastatic renal cancer: a University of Chicago Phase II Consortium Study. J Clin Oncol 2000;18:371 – 5.

46. Raje N, Kumar S, Hideshima T, et al. Seliciclib (CYC202 or R-roscovitine), a small-molecule cyclin-dependent kinase inhibitor, mediates activity via down-regulation of *Mcl-1* in multiple myeloma. Blood 2005; 106:1042 – 7.

47. Leclerc S, Garnier M, Hoessel R, et al. Indirubins inhibit glycogen synthase kinase-3β and CDK5/P25, two protein kinases involved in abnormal τ phosphorylation in Alzheimer's disease. A property common to most cyclin-dependent kinase inhibitors? J Biol Chem 2001;276: 251 – 60.

48. Zarkowska T, Mittnacht S. Differential phosphorylation of the retinoblastoma protein by G_1/S cyclin-dependent kinases. J Biol Chem 1997;272:12738 – 46.

49. Rudek MA, Bauer KS, Lush RM, et al. Clinical pharmacology of flavopiridol followed by a 72-hour continuous infusion. Ann Pharmacother 2003;37:1369 – 74.

50. Fischer PM, Gianella-Borradori A. CDK inhibitors in clinical development for the treatment of cancer. Expert Opin Investig Drugs 2003;12: 955 – 70.

51. Shapiro GI. Cyclin-dependent kinase pathways as targets for cancer treatment. J Clin Oncol 2006;24:1770 – 83.